PIV Investigation of the 3D Instantaneous Flow Organization behind a Micro-ramp in a Supersonic Boundary Layer

Z. Sun, F.F.J. Schrijer, F. Scarano, and B.W. van Oudheusden

1 Introduction

Shock wave boundary layer interaction (SWBLI) is a flow phenomenon that is critical for many high speed applications, such as supersonic inlets and propulsion-wing or -fuselage interactions. Much effort has been devoted to investigate the mechanism of SWBLI, its turbulent nature and the role of large-scale fluctuations[1]. Different types of flow control techniques have been proposed to alleviate the adverse effects introduced by SWBLI, such as flow separation and fluctuating pressure loads. Micro-ramp vortex generators are considered to be a preferred type of passive boundary layer control technique, due to a limited increase in drag compared to conventional larger vortex generators that emerge outside the boundary layer, while still being effective in reducing flow separation.

Using the geometry that follows the optimization study performed by Anderson et al[2], the working principle of a micro-ramp has been investigated through both experimental and numerical approaches. A mean flow description by Babinsky et al[3] depicts the streamwise counter rotating vortex pair and other secondary vortices in streamwise direction. Using these observations a general working mechanism of the micro-ramp was deduced: the boundary layer is energized by the high momentum fluid in the free stream entrained by the downwash caused by the streamwise primary vortex pair. This results in a fuller boundary layer profile, which is more capable of enduring the adverse pressure gradient induced by incident shock waves or compression ramps. However, due to the strong three-dimensionality of the flow past the micro-ramp, the instantaneous flow structure is rather different from the one obtained in the mean sense. Blinde et al[4] identified several vortex pairs developing downstream of a micro-ramp array through stereo-PIV in two planes parallel to the surface at different heights. These vortex pairs were suggested to be cross sections of legs of hairpin vortices similar to those that naturally occur

Z. Sun · F.F.J. Schrijer · F. Scarano · B.W. van Oudheusden
Faculty of Aerospace Engineering, Delft University of Technology
Kluyverweg 1, 2629 HS, Delft (The Netherlands)

in a turbulent boundary layer. Based on their observations Blinde et al formulated a conceptual model of a train of hairpin vortices developing downstream of each micro-ramp. An LES simulation of the flow past a single micro-ramp performed by Li et al[5] visualized a series of vortex elements behind the trailing edge. The structure of these vortices only partly confirms the model obtained from Blind et al's experiment. In fact the legs of the vortices in the computations of Li et al do not appear to align with the wall like hairpins proposed by Blinde. Instead, they rather appear to have a ring shape belonging to a plane slightly inclined to the wall normal direction. In their paper, Li et al concluded that the vortices are connected also on the bottom side therefore featuring full rings. The structure of the upper part of the wake has also been confirmed by a recent experimental research performed by Lu et al[6] using laser sheet visualization. The visualizations revealed a pronounced Kelvin-Helmholtz instability developing downstream of micro-ramps. According to the explanation by Lu et al, the KH instability structures develop as a secondary instability of the streamwise vortex pair, which is more stable in the region near the micro-ramp and breaks down downstream. This latter description is in contrast with the previous two where no mention is made of the interaction between the streamwise vortices and the hairpin- or ring-shaped rollers formed at the wake interface.

Since the results from experimental and numerical approaches partially agree on the appearance of the intermittent vortices and their relation with the streamwise vortices, the present experimental research aims at visualizing the controversial vortices and identifying their origin. Tomographic-PIV (Elsinga et al[7]) is chosen for the reason that it offers the capability of detecting instantaneous patterns in a complex three-dimensional flow.

2 Experimental Arrangement

Experiments were carried out in the blow-down supersonic wind tunnel ST15 of Delft University of Technology. The wind tunnel was operated at Mach 2.0 (free stream velocity U_{ref}=532 m/s), with a stagnation pressure of P_0=3.2 bar. The boundary layer developing along the tunnel bottom wall was selected for the micro-ramp investigation. After developing for approximately 1.0 m past the throat section of the nozzle, the boundary layer reaches a thickness of 4.8 mm.

The investigated micro-ramp height is 4 mm, the geometry follows that proposed in the study of Anderson et al[2] resulting in a chord length of 27.4 mm and a spanwise width of 24.4 mm. Tomo-PIV measurements were carried out within two volumes starting 35 mm downstream of the micro-ramp of $25\times15\times6$ mm^3 size. The layout of the two measurement volumes is schematically depicted in figure 1.

The flow was seeded by DEHS droplets with a diameter of approximately 1 μm. The tracers were injected into the flow through a seeding device placed upstream of the settling chamber. According to the study of Ragni et al[8] the DEHS particle tracers have a relaxation time of approximately 2 μs, which enable accurate tracking of flow structures down to 1 mm. The seeded flow was illuminated by a Spectra-Physics Quanta Ray PIV-400 double pulse Nd:Yag laser at a wavelength of 532 nm.

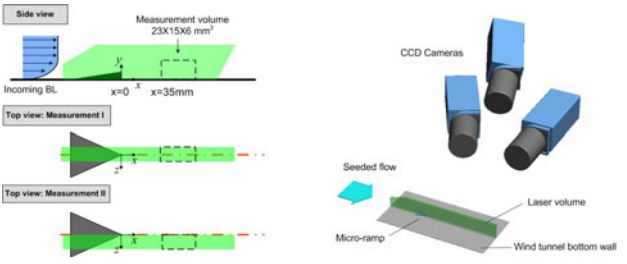

Fig. 1 left: arrangements of the two measurement volumes; right: camera positions with respect to laser volume and micro-ramp.

Each pulse has energy of 400 mJ and duration of 6 ns. A laser probe was inserted from the side wall downstream of the test section, through which the laser beam was shaped into a volume of 6 mm thickness.

Three PCO Sensicam QE CCD cameras with a sensor of 1376×1040 pixels were equipped with Nikon 105 mm objectives (see figure 1) set at numerical aperture of $f_{\#}$=11, 11 and 9 respectively and the Scheimpflug principle was applied. Two cameras were viewing from upstream to take the benefit of the forward light scattering of the particles. The laser pulse separation time was selected at 0.6 μs and image pairs were recorded at a rate of 5 Hz. A digital image resolution of 43.7 pixel/mm was achieved with a particle displacement of 14 pixels in the free stream. 400 images were recorded for each volume to achieve data convergence.

3 Results and Anlysis

3.1 Mean Flow Characteristics

Previous studies on micro-ramp flow reveal that a streamwise counter rotating vortex pair symmetric to the center plane (z=0) dominates the mean flow field. Contour plots of u-component shown in figure 2 are extracted to represent the mean flow structure. One of the pairing vortices can be observed through the vectors overlaid

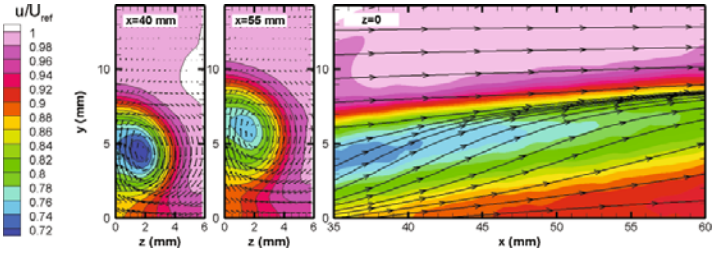

Fig. 2 Selected contour plots of the mean flow field from Measurement II.

on the $y-z$ plane contours. An additional proof of the vortices is provided by the streamline pattern in the center plane, which is the footprint of the central upwash induced by the vortices.

Another significant phenomenon revealed through figure 2 is the wake region of low streamwise momentum that encompasses the streamwise vortices. Assuming the flow axisymmetric, the wake is expected to obtain a smooth circular shape. Along its streamwise movement, the wake is lifted and also expands. A shear layer following the wake configuration is located at the edge, where the streamwise velocity is reduced from U_{ref} to approximately $0.8U_{ref}$ near the core region at this distance behind the micro-ramp element.

3.2 Turbulent Characteristics

The distributions of the two fluctuation components, $\langle u' \rangle$ and $\langle v' \rangle$, in the center plane ($z = 0$) shown in the left part of figure 3 reveal a similar shear layer structure with higher fluctuations at the center and lower fluctuations at both edges.

Profiles of the turbulent components and averaged streamwise velocity at $x = 40$ mm are shown in the right part of figure 3. From the streamwise velocity profile, the wake is composed of the upper and lower shear layers, within which $\langle u' \rangle$ and $\langle v' \rangle$ exhibit considerable increase and the maxima are reached in the upper shear layer. The positions of turbulent maxima do not exactly coincide for the two components. Also, $\langle v' \rangle$ is larger than $\langle u' \rangle$ in the center region of the wake, which suggests anisotropy of the turbulent fluctuations.

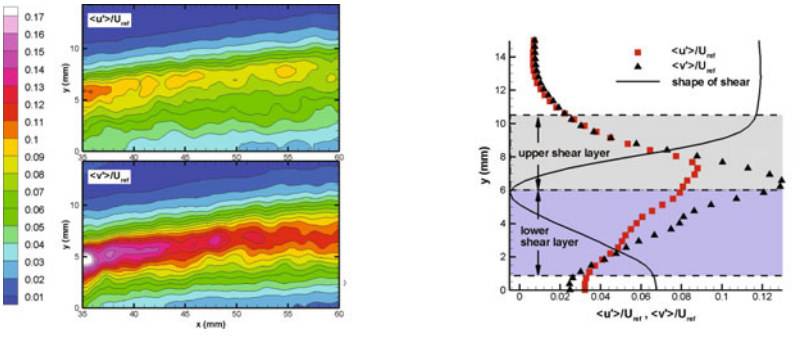

Fig. 3 Fluctuation velocity distributions, left: contour plots of $\langle u' \rangle$ (up) and $\langle v' \rangle$ (down) at center plane; right: fluctuation and averaged streamwise velocity profiles at $x = 40$ mm of the center plane.

3.3 Cross-Sectional Representations

To assist the interpretation of the instantaneous flow structure, figure 4 shows three cross-sectional contours of u-component, two in $y-z$ plane at $x = 42$ mm and

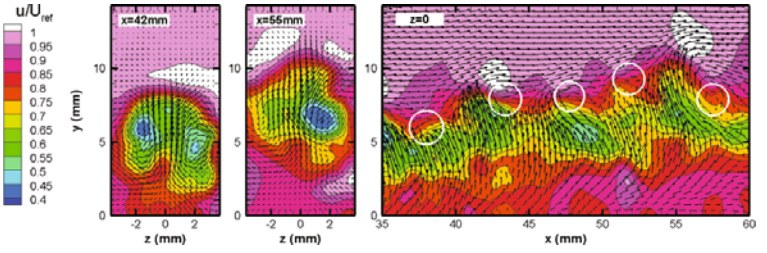

Fig. 4 Selected contour plots of the instantaneous flow field from Measurement I.

55mm and the third in $x-y$ plane at $z=0$, extracted from an instantaneous three-dimensional flow field from Measurement I.

The dominating streamwise vortex pair is revealed in the $y-z$ planes. Its appearance is not as symmetric to the center plane as observed from the mean flow field, suggesting an instantaneous meandering behavior. Also, the wake exhibits a modulated edge, whereas it is a smooth and axisymmetric in the mean flow.

The wavy velocity interface of the wake edge visualized in the $x-y$ plane can be understood as the imprint of a Kelvin-Helmholtz instability of the shear layer. After subtracting a constant value from the vector field, the KH vortices are visualized, which are indicated by the white circles in the contour plot. Due to their clockwise rotational direction these vortices induce local regions of increased and decreased velocity on the upper and lower sides of the vortices, respectively. It may be noted that the areas with high streamwise velocity on top of the wake in the $y-z$ contours are intersections of such high speed regions.

3.4 Volumetric Representations

The instantaneous three-dimensional structure, as obtained from the Tomo-PIV measurements, is characterized by means of velocity and vorticity iso-surfaces, as shown in figure 5. These volumetric renderings relate to the same flow realization as the cross-sectional flow fields in figure 4. Two values of the u-component are displayed: high speed in pink ($1.02U_{ref}$) and low speed in green ($0.8U_{ref}$), which correspond to high and low speed regions induced by the KH vortices. Both regions are separate in space and exhibit a typical intermittency similar to the one observed in KH instability.

The vorticity representations reveal both the primary streamwise vortex pair and the KH vortices simultaneously. The streamwise vortices are visualized through ω_x in different colors, because of their opposite rotational directions. The intermittent KH vortices are presented though ω_z, which explains why only the top part of the KH vortices is visualized, while an arc shape can be expected for the KH vortices which follow the shape of the instantaneous shear layer in $y-z$ cross section.

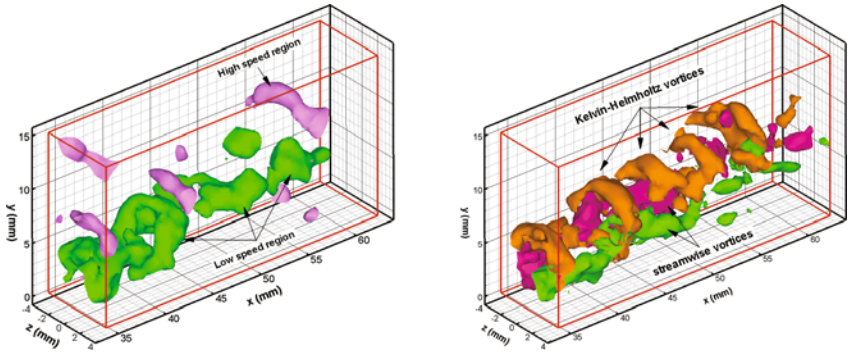

Fig. 5 Volumetric representation, left: iso-surfaces of *u*-component; right: iso-surfaces of vorticity.

4 Conclusions and a Conceptual Model

An experimental study has been carried out to investigate the instantaneous organization of the three-dimensional micro-ramp flow using Tomo-PIV. As a result, a few conclusions can be drawn.

The streamwsie vortex pair and the arc-shaped Kelvin-Helmholtz vortices exist simultaneously in the wake of the micro-ramp, thus a two-type vortex flow model (illustrated in figure 6) can be summarized. These two categories of vortices are generated out of different mechanisms, the streamwise vortex pair is produced by the chamfered side edges of micro-ramp, while the arc-shaped vortices are caused by the KH instability at the interfacial shear layer between the wake and free stream. The streamwise vortex pair makes the major contribution to the control effectiveness, however, the impact of the KH vortices towards SWBLI requires further investigation.

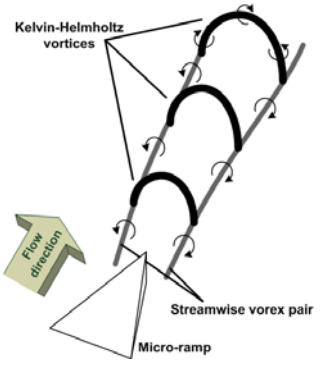

Fig. 6 A conceptual model of the instantaneous vorticity structure.

References

1. Dolling, D.S.: Fifty years of shock-wave/boundary-layer interaction research: What next? AIAA J. 39(3), 1517–1531 (2001)
2. Anderson, B.H., Tinapple, J., Surber, L.: Optimal control of shock wave turbulent boundary layer interactions using micro-array actuation. AIAA Paper 2006–3197 (2006)
3. Babinsky, H., Li, Y., Pitt Ford, C.W.: Microramp control of supersonic oblique shock-wave/boundary-layer interactions. AIAA J. 47(3), 668–675 (2009)
4. Blinde, P.L., Humble, R.A., van Oudheusden, B.W., Scarano, F.: Effects of micro-ramps on a shock wave/turbulent boundary layer interaction. Shock Waves J. 19(1), 507–520 (2009)
5. Li, Q., Liu, C.: LES for supersonic ramp control flow using MVG at $M = 2.5$ and $Re_\theta = 1440$. AIAA Paper 2010–592 (2010)
6. Lu, F.K., Pierce, A.J., Shih, Y.: Experimental study of near wake of micro vortex generators in supersonic flow. AIAA Paper 2010–4623 (2010)
7. Elsinga, G.E., Scarano, F., Wieneke, B., van Oudheusden, B.W.: Tomographic particle image velocimetry. Exps. Fluid 41(6), 933–947 (2006)
8. Ragni, D., Schrijer, F., van Oudheusden, B.W., Scarano, F.: Particle tracer response across shocks measured by PIV. Exps. Fluid 50(1), 53–64 (2011)